Journal of Molecular Structure 1330 (2025) 141490

Contents lists available at ScienceDirect

Journal of Molecular Structure

journal homepage: www.elsevier.com/locate/molstr

Cyclobutylamino-naphthalimide-based fluorescent probe for detection of glutathione in living cells

Samarpita Das [a], Pooja Goswami [b], Harish K. Indurthi [a], Biplob Koch [b], Deepak K. Sharma [a,*]

[a] Department of Pharmaceutical Engg. and Tech., IIT-Banaras Hindu University, Varanasi, UP 221005, India
[b] Genotoxicology and Cancer Biology Laboratory, Department of Zoology Institute of Science, Banaras Hindu University, Varanasi, UP 221005, India

ARTICLE INFO

Keywords:
cyclobutylamino-naphthalimide ratiometric probe detection GSH biosafety fluorescence imaging

ABSTRACT

Fluorophores that incorporate cyclobutylamine auxochromes exhibit improved quantum yields, photostability, biocompatibility, and cell permeability. In this study, we present the design and synthesis of a novel ratiometric probe (**NAPB**) based on cyclobutylamino-naphthalimide (**NCB**), which enables the selective and sensitive detection of glutathione (GSH). **NAPB** employs a nucleophilic substitution/cyclization strategy to detect GSH. In the presence of GSH, a noticeable ratiometric change in the emission wavelength occurs, shifting from blue to greenish-yellow fluorescence. The probe can detect GSH rapidly, with a detection limit as low as 39.1 nM. Following confirmation of biosafety through an MTT assay, NAPB was further utilised for fluorescence imaging of GSH in live HepG2 cells.

1. Introduction

Glutathione (GSH) is a key member of the reactive sulfur or thiol family and showcases a multitude of physiological functions, such as regulation of oxidative stress, immune responses, detoxification and gene regulation [1–3]. GSH plays a crucial role in protecting cellular components against oxidative damage via the action of GSH peroxidase (GPx). GSH undergoes a reduction in the presence of NADPH by the catalytic activity of the enzyme GSH reductase. Two such reduced molecules of GSH undergo oxidation by GPx to form GSH disulfide (GSSG). This process initiates a redox cycle that reduces hydrogen peroxide (H_2O_2) to water and molecular oxygen via a redox cycle which helps to maintain cellular homeostasis [4–6]. Due to its reducing properties, GSH forms conjugates with toxic reactive metabolites of xenobiotics, effectively aiding in their removal from the body. An imbalance in GSH levels can lead to serious health issues, contributing to various physiological conditions such as AIDS, leukopenia, neurodegenerative diseases, cancer, HIV, liver injury, and other ailments. Therefore, developing effective tools and methods for the selective and sensitive detection of GSH is critical for facilitating early clinical diagnosis and conducting preliminary research. Several high-technology instruments, such as mass spectrometry (MS), high-performance liquid chromatography (HPLC), HPLC-MS/MS, capillary electrophoresis, etc., have been applied for the detection and quantification of GSH. Recently, fluorescence-based analytical techniques have attracted the attention of chemical analysts as a sensitive, noninvasive, and high-resolution alternative for GSH detection with the benefits of real-time monitoring in living systems. Several fluorescent probes have been developed to date to monitor GSH [7–15]. However, most are based on common fluorophores with sub-par photophysical (high quantum yield, improved brightness) and physicochemical properties (stability, cell permeability). In our recent studies, [16,17] we have demonstrated that cyclobutylaminated fluorophores have higher quantum yields, better photostability, excellent biocompatibility and decent cell permeability.

Herein, we demonstrate the application of cyclobutylaminated naphthalimide in the design and synthesis of a novel ratiometric fluorescent probe (**NAPB**) for the efficient detection of GSH (Fig. 1). **NAPB** is comprised of cyclobutylaminated naphthalimide **(NCB)** as the main fluorophore, attached to a chloroacetyl unit which is meant for the recognition of GSH. Since thiols possess excellent nucleophilicity, they could undergo a simple SN_2 nucleophilic substitution with the chlorine atom of the acetyl moiety, followed by a nucleophilic attack of the free amino group of GSH on the carbonyl of the response unit, thereby dissociating it and releasing the parent fluorophore. The acetyl group, in turn, would undergo intramolecular cyclization with GSH and form an adduct with the latter. After synthesis of the **NAPB**, we plan to check its sensitivity and selectivity to GSH and also explore further its potential applications in the imaging of GSH in living cells.

* Corresponding author.
E-mail address: deepak.phe@itbhu.ac.in (D.K. Sharma).

https://doi.org/10.1016/j.molstruc.2025.141490
Received 29 July 2024; Received in revised form 7 December 2024; Accepted 17 January 2025
Available online 21 January 2025

2. Results and discussion

Commercially available precursor 4-bromo-1,8-naphthalic anhydride (**A**) was refluxed with *n*-butyl-amine in ethanol for 2 h to yield intermediate **B** in 75 %. Intermediate **B** then undergoes aromatic substitution with cyclobutylamine in the presence of triethylamine (Et_3 N) as base and dimethylsulfoxide (DMSO) as solvent for 6 h to afford **NCB** in 78 % yield [17]. After its synthesis, **NCB** was subjected to simple nucleophilic substitution with 2-chloroacetyl chloride in the presence of a strong base under reflux conditions within a short period of 2 h to afford the probe **NAPB** in moderate yields of 76 %. (Scheme 1) The chemical structure of new target molecule was well characterized by the standard spectroscopic techniques such as NMR and MS spectroscopies (see the Supporting Information). The LC-MS analysis of probe **NAPB** showed m/z for M + H^+ at 399.1681 and 401.1819.

We examined **NAPB** (1.25 μM) in the presence of an equimolar amount of GSH under slightly basic conditions (pH 8.5) and at ambient temperature. Within 5 to 10 min, we observed a change in fluorescence from blue to greenish-yellow in a thin layer chromatogram (TLC) under UV light irradiation (λ_{ex}: 365 nm). After 30 mins, LC-MS analysis of the reaction mixture of **NAPB** and GSH was performed. The results indicated the complete disappearance of **NAPB** (m/z for M + H^+: 399.1681, 401.1819) and formation of **NCB** (m/z for M + H^+: 323.1933) along with a corresponding cyclization product for GSH (**GA**) (m/z for M + H^+: 348.8954) (Scheme 2**a**) (See Supporting information). A similar observation was made when **NAPB** was subjected to an equimolar amount of Cysteine (Cys) under the same conditions as GSH, where the reactivity of probe to thiol was ensured by the formation of **NCB** and corresponding cyclization product for Cys (**CA**) (m/z for M + H^+: 162.9741) (**Scheme 2b**). Next, we hypothesized that in the presence of other thiol-sensitive reactive species, **NAPB** would remain unchanged due to the potential interaction of GSH with the thiol-reactive site. To test this, we mixed **NAPB** with an equimolar mixture of GSH and N-propylmaleimide (NPM), a well-known Michael-acceptor that is extremely susceptible to reaction with thiols. To our delight, we detected the formation of an NPM-GSH conjugate **(GNA)** (m/z for M + H^+: 491.3078) along with the preservation of **NAPB** (m/z for M + H^+: 391.3051), which showcases the selective interaction of the probe to GSH (Scheme 2**c**). Furthermore, we confirmed the selectivity of **NAPB** for biothiols by subjecting it to an equimolar mixture of GSH and Cys (1:1). After one hour of incubation with the GSH:Cys mixture, LC-MS analysis showed the formation of **GA**, but no molecular ion peak corresponding to **CA** was detected. Such selectivity of **NAPB** towards GSH can be due to the priority in the formation of GSH cyclization product **(GA)** as compared to Cys-cyclization product **(CA).** This can be attributed to the higher nucleophilicity of the GSH in addition to the structural properties of the sensing group which includes the reactivity of the halogen atom and the optimal length of the carbon chain [14].

The photophysical behaviour of the probe **NAPB** (1.25 μM) was determined in phosphate buffer (mixed with DMSO in a volumetric ratio of 8:2, and maintained at pH 8.5) (Fig. 2). An analysis of the absorption spectrum revealed a broad absorption band for **NAPB**, characterized by a notable absorbance peak at 345 nm. After introducing glutathione (GSH) in a stoichiometric ratio of 1 equivalent (dissolved in PBS), the absorption spectrum exhibited a significant redshift, with the peak moving from 345 nm to 445 nm. This spectral shift is indicative of the cleavage of **NAPB** in the presence of GSH and the corresponding release of the original fluorophore form, designated as **NCB**. In addition to the absorption changes, the fluorescence characteristics of **NAPB** were evaluated. The probe displayed an emission band centered around 451 nm, producing a vibrant blue fluorescence when excited at 345 nm. However, upon the addition of GSH (1 equiv.), the emission spectrum underwent a redshift, with the peak now appearing at 549 nm, which is aligned with the emission characteristics of **NCB**. Consequently, this transition results in the emission of a yellowish-green fluorescence. This behaviour creates a distinctive ratiometric response for probe **NAPB** in the presence of GSH, providing a valuable tool for detecting and quantifying changes in glutathione levels in biological systems.

Subsequently, the fluorescent titration of probe **NAPB** (1.25 μM in phosphate buffer mixed with DMSO in a ratio of 8:2, pH 8.5) with GSH solution in PBS (0–20 equiv.) was investigated. The results unequivocally demonstrate that the introduction of GSH to the probe solution causes a significant decrease in the fluorescence intensity of the emission band at 451 nm, while concurrently enhancing the emission band at 549 nm, when subjected to excitation at 345 nm and 445 nm, respectively (Fig 3a–3b). The plotted fluorescent intensities at 451 nm and 549 nm against the varying GSH concentrations (0–20 equivalents), depicted in Fig. 3c, reveal a marked decline in blue fluorescence emission (F_{445}) alongside a pronounced increase in yellowish-green fluorescence (F_{549}) up to a GSH concentration of 10 equivalents, after which the probe reaches saturation. This indicates a concentration-dependent response of **NAPB** to GSH. A strong linear correlation was established between the fluorescence intensity ratio (F_{549}/F_{451}) of probe **NAPB** and GSH concentration within the range of 0 to 10 equivalents (R^2 = 0.993).

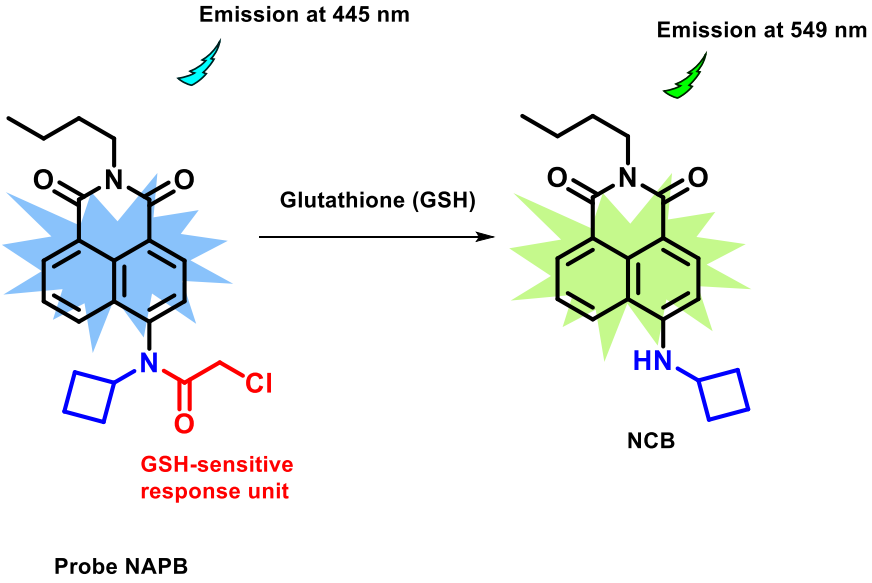

Fig. 1. Chemical structure and GSH-sensing mechanism of probe **NAPB**.

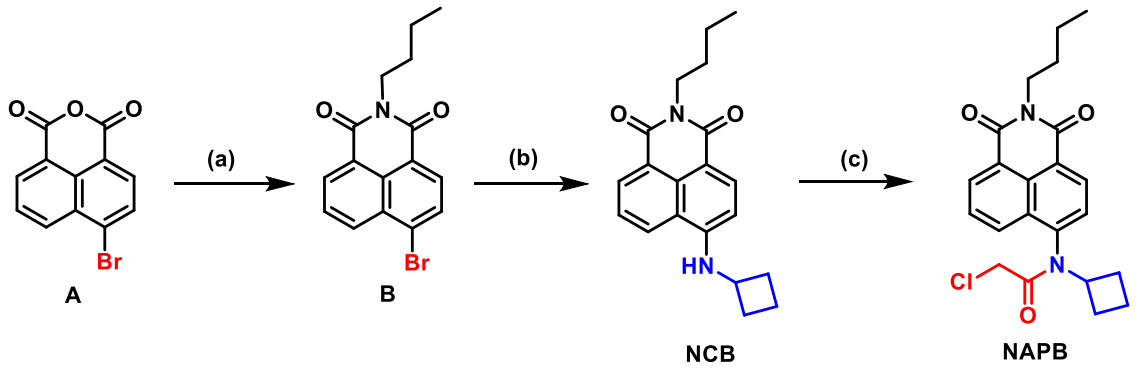

Scheme 1. Synthesis of NAPB from NCB.
[a]**Reagents and conditions**: (a) **A** (3 mmol), *n*-butylamine (1.5 equiv.), EtOH (5 mL), refluxed at 80 °C for 2 h, 75 %; (b) **B** (0.3 mmol), triethylamine (1.5 equiv.) and cyclobutylamine (1.5 equiv.), DMSO (2 mL), heated at 110 °C for 6 h, 78 %; (c) **NCB** (0.5 mmol), chloroacetyl chloride (5 eq.), dried Na_2CO_3 (2 eq.), ACN (3 mL), refluxed at 80 °C for 2 h, 76 %.

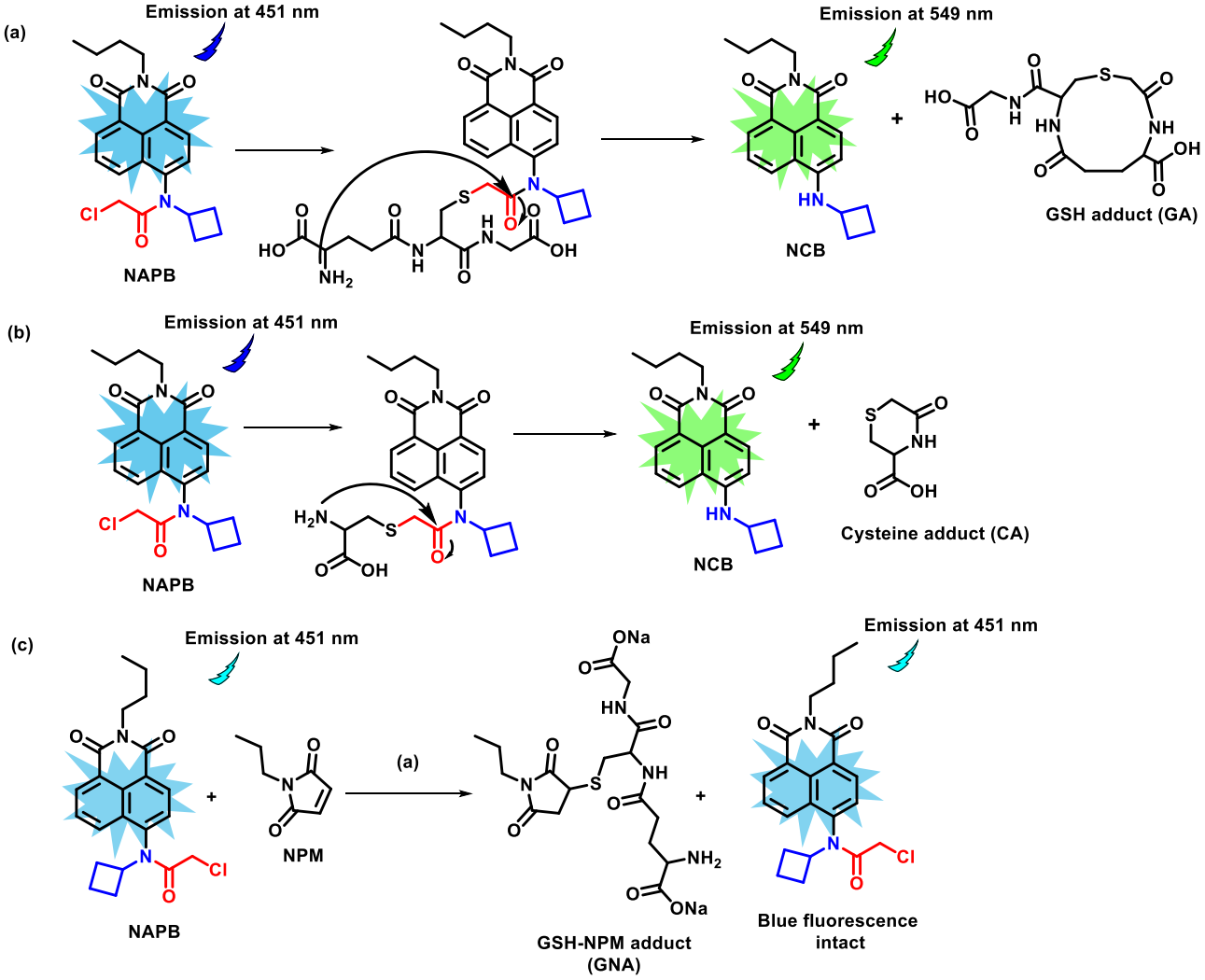

Scheme 2. Nucleophilic reactions of probe NAPB.[a]
[a]**Reagents and Conditions. (a) NAPB** (0.012 mmol) in DMSO, GSH (1 equiv.) and Na_2CO_3 (cat.) in water (pH=8.5), rt, 30 mins; **(b) NAPB** (0.012 mmol) in DMSO, Cys (1 equiv.) and Na_2CO_3 (cat.) in water (pH = 8.5), rt, 30 mins; **(c)** NPM (1 equiv.), GSH (1 equiv.), Na_2CO_3 (1.5 equiv.) in water, stirred for 10 mins, **NAPB** (0.012 mmol) in DMSO, rt, 30 mins.

Furthermore, the detection limit was determined to be as low as 39.1 nM, calculated using the formula 3δ/K, where δ signifies the standard deviation of blank measurements, and K denotes the slope of the plot of fluorescence intensity *versus* sample concentration (Fig. 3d).

To evaluate the time-dependent response of the probe towards the detection of GSH, **NAPB** was subjected to a fixed concentration of GSH

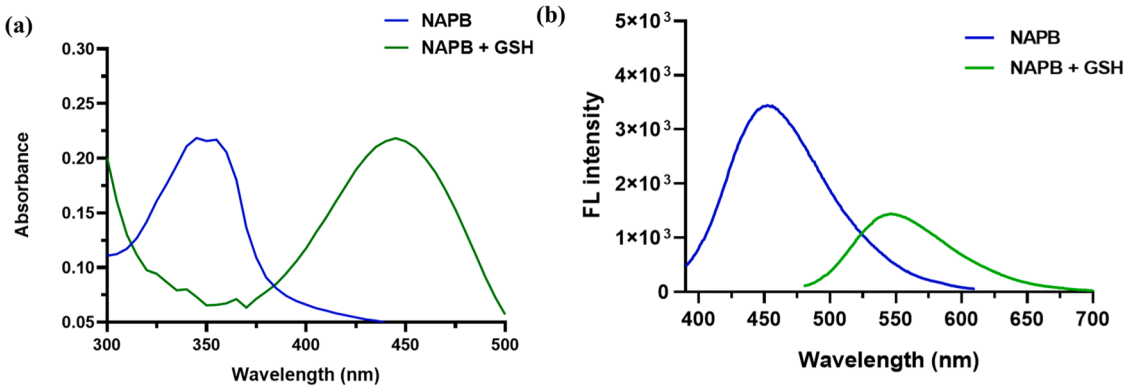

Fig. 2. UV–Vis absorption spectra **(a)** and fluorescence emission spectra **(b)** of **NAPB** (in phosphate buffer mixed with DMSO in a ratio of 8:2, pH 8.5) before and after the addition of **Glutathione (GSH)** (1 equiv. in PBS) (λ_{ex}: 345 nm and 445 nm).

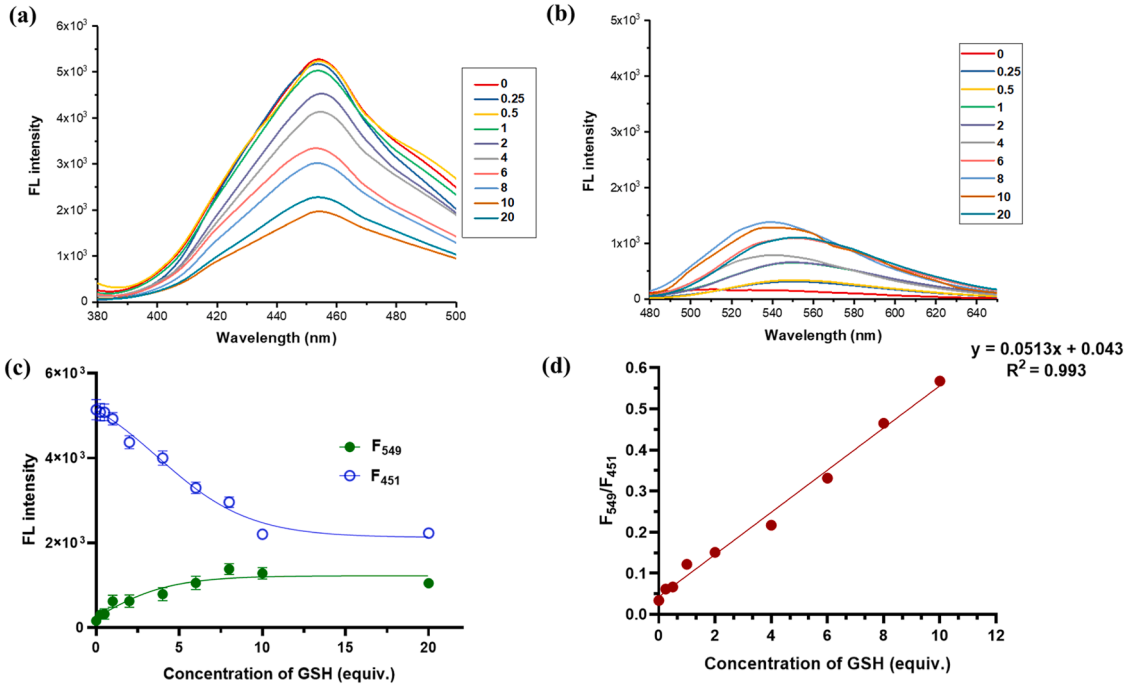

Fig. 3. Fluorescence responses of **NAPB** (1.25 μM) to various concentrations of GSH (0 - 20 equiv.) when excited at λ_{ex} = 345 nm **(a)** and λ_{ex} = 445 nm **(b)**, respectively; **(c)** Fluorescence intensities of **NAPB** (1.25 μM) at 451 nm and 549 nm in response to increasing concentrations of GSH (0–20 equiv.) when excited at λ_{ex} = 345 nm and λ_{ex} = 445 nm, respectively; **(d)** GSH concentration-based response curve of **NAPB** shows linear relationship within a concentration range of 0 −10 equiv.

(1 equiv.) for an hour. The addition of GSH to the probe led to immediate enhancement of fluorescence emission at 549 nm within about 5–10 mins which enhanced further with time and reached equilibrium after 35 mins (Fig. 4a). This analysis demonstrated that the chloride of **NAPB** was rapidly replaced by the thiol group of GSH, and subsequently, the ester bond was attacked by the intramolecular $-NH_2$ group to free the fluorescent core in about 5–10 mins. When subjected separately to varying concentrations of GSH (0–10 equiv.) to verify the time-dependent behaviour of **NAPB** (1.25 μM), it showed initial fluorescence response at 549 nm within 10 min of GSH introduction at all possible concentrations and equilibrium is reached after about 35–40 mins of exposure in every case (Fig. 4b). This demonstrates a rapid reaction time and consistent response of **NAPB** to GSH.

The selectivity study of **NAPB** towards GSH was conducted in the presence of various interfering species, such as ions (Na^+, K^+, Fe^{3+}, Cl^-, HCO_3^-, etc.), amino acids (Glu, Gly, His, Arg, etc.), reactive oxygen species ($ONOO^-$, H_2O_2, etc.) as well as other thiol species (Cys, *N*-Ac-Cys). As illustrated in Fig. 4c, **NAPB** displayed the highest fluorescence intensity ratio (F_{549}/F_{445}) in presence of GSH, followed by Cys and *N*-Ac-Cys, in comparison to other interfering ionic species, amino acids or ROS. This finding highlights the selectivity of NAPB for biothiols, particularly GSH, as the intensity ratio (F_{549}/F_{445}) was approximately 2.02 times and 4.05 times greater than that for Cys and N-Ac-Cys, respectively. pH stability of such fluorescent sensors requires extensive pH stability, especially in the physiological range for their *in vitro* and *in vivo* applications. We thus evaluated the stability of **NAPB** to changes in the physiological pH range (4–8), and to our utter delight, we found that **NAPB** shows excellent stability (Fig. 4d).

Encouraged by the selectivity, sensitivity, and pH stability of the probe, we proceeded to assess its application for the detection and imaging of GSH in living cells. Prior to imaging, we evaluated the biocompatibility of **NAPB** in various cancer cell lines (HepG2, HCT116, and MCF-7) using the MTT assay technique. We measured the relative rates of cellular growth in these cancer cells incubated separately with

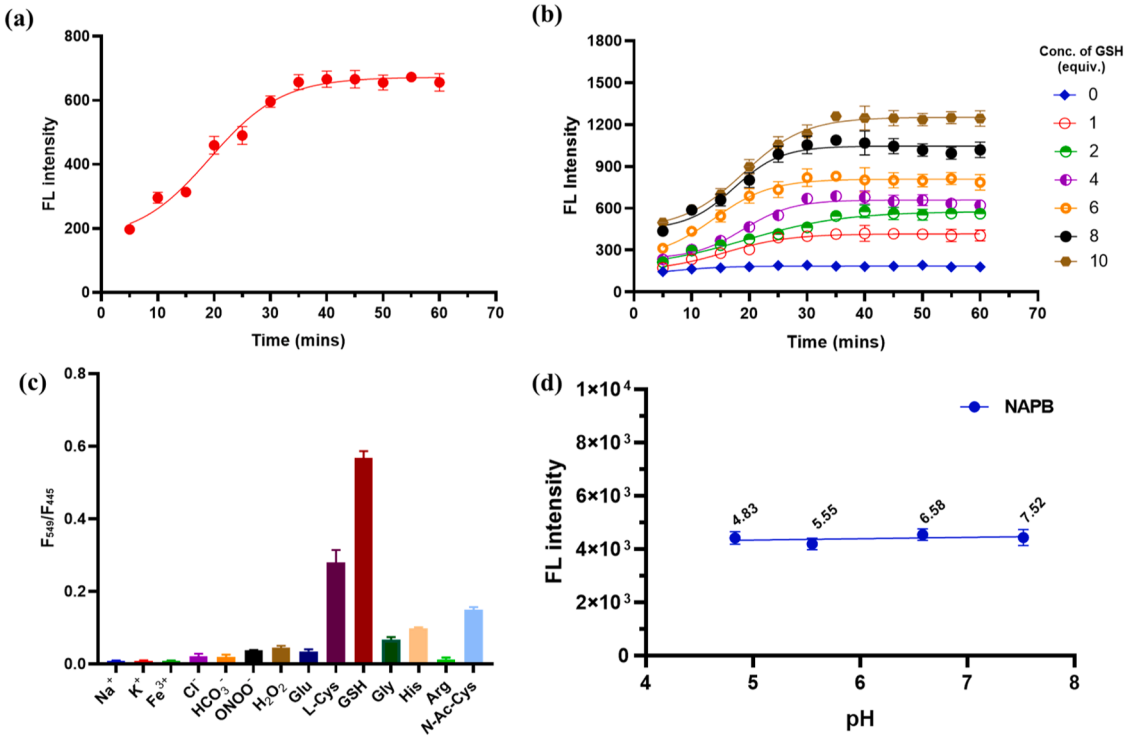

Fig. 4. **(a)** Time-dependent fluorescence response of **NAPB** (1.25 μM) to a fixed concentration of GSH (1 equiv.) at 549 nm (λ_{ex}: 445 nm); **(b)** Time-dependent fluorescence response of **NAPB** (1.25 μM) to variable concentrations of GSH (0–10 equiv.) at 549 nm (λ_{ex}: 445 nm); **(d)** Evaluation of the stability of probe **NAPB** (1.25 μM) to changes in pH (4–8) at λ_{em} = 549 nm (λ_{ex}: 445 nm).

NAPB at concentrations ranging from 1 to 10 μM over 24 h. As shown in Fig. 5a, the percentage of cell viability at lower concentrations (1–5 μM) remained at or above 90 % across all three cell lines. However, as the concentration of NAPB increased, cellular viability declined, dropping to as low as 80 % in the HepG2 and HCT116 cell lines at a concentration of 10 μM. For MCF-7 cells, cell viability decreased to approximately 60 % at the same concentration of **NAPB**. Based on the findings from the biocompatibility assay, we concluded that the probe is safe for use in living systems at a concentration of 5 μM.

For fluorescence imaging of GSH in living cells using the probe (Fig. 5b), HepG2 cells were incubated with **NAPB** before being treated with exogenous GSH, along with a control compound, **NPM**, to confirm the probe's selectivity for GSH. As depicted in the figure tiles (v-viii), the cells treated with **NAPB** (5 μM) exhibited bright blue fluorescence

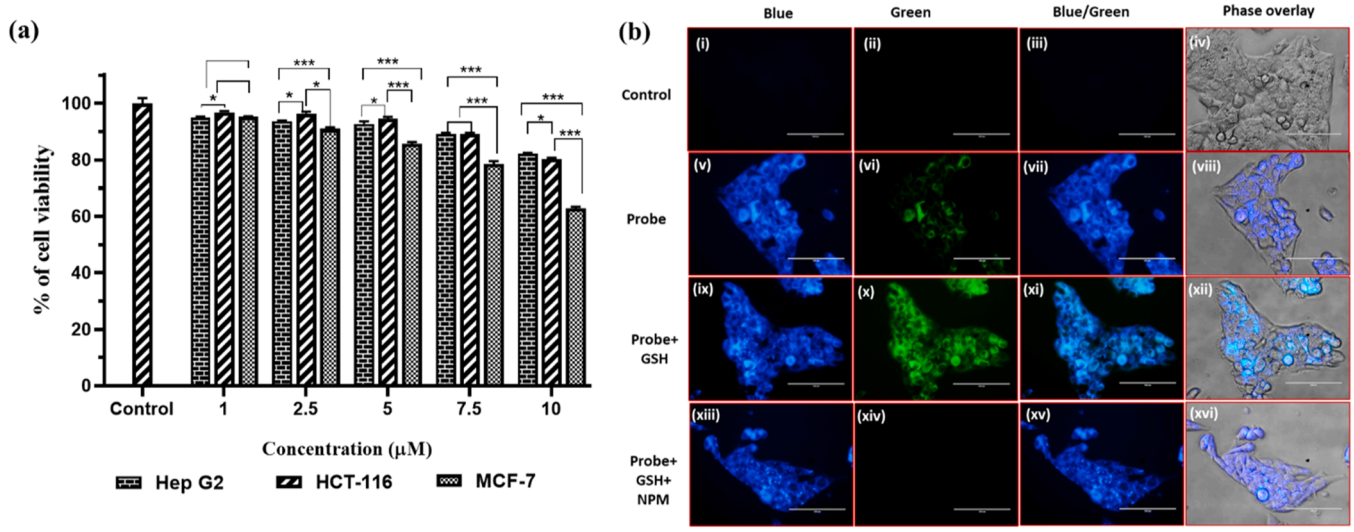

Fig. 5. **(a)** Measurement of percent viability of HepG2 liver cancer cells, HCT116 colorectal cancer cells and MCF-7 breast cancer cells, each incubated with probe **NAPB** at various concentrations ranging from 1 μM to 10 μM using MTT assay. Statistical analysis has been done by One-way ANOVA followed by Tukey's P test with multiple comparisons and the level of significance $*p < 0.05$, $**p < 0.01$ and $***p < 0.001$; **(b)** Fluorescent and merged images of HepG2 cells when treated with probe **NAPB** in the absence and presence of exogenous GSH and NPM; (i-iv) Control, (v-viii) Cells were treated with probe **NAPB** (5 μM) only for 1 h and then the image was captured, (ix-xii) Cells were treated with probe **NAPB** (5 μM) only for 1 h, followed by GSH (5 μM) for 30 mins and then image was captured, (xiii-xvi) Cells were treated with probe **NAPB** (5 μM) only for 1 h, followed by a mixture of GSH:NPM (5 μM each) for 30 mins and then image was captured. λ_{ex}: 357–344 and 470 nm, and λ_{em}: 447–460 and 510–542 nm. Scale bar = 100 μm.

emission in the blue channel (λ_{ex}: 357–344 nm and λ_{em}: 447–460 nm), while only a faint fluorescence was observed in the green channel (λ_{ex}: 470 nm and λ_{em}: 510–542 nm), indicative of a lower concentration of endogenous GSH. However, upon incubation of the probe-treated cells with exogenous GSH (5 μM) for an additional 30 min (figure tiles ix-xii), a significant increase in green fluorescence intensity was recorded, attributed to the cleavage of **NAPB** into the parent fluorophore **NCB** (λ_{em}: 549 nm) in the presence of GSH. Furthermore, when HepG2 cells that had been pre-treated with **NAPB** (5 μM) for one hour were subjected to a mixture of exogenous GSH (5 μM) and the control compound **NPM** (5 μM) for 30 min (figure tiles xiii-xiv), the green fluorescence completely diappeared. This finding suggests that free GSH was effectively removed from the cells through interaction with NPM, leaving the probe intact, which emitted fluorescence solely at 451 nm.

3. Conclusion

In conclusion, we have successfully synthesized a novel ratiometric probe, designated as **NAPB**, which is based on an enhanced light-emitting fluorophore, specifically cyclobutylamino-functionalised naphthalimide (**NCB**), for the selective and sensitive detection of glutathione (GSH). **NAPB** employs a straightforward methodology involving nucleophilic substitution followed by cyclization for GSH detection. Control experiments conducted in the presence of NPM further confirm the selectivity of **NAPB** towards GSH. The probe demonstrates a ratiometric change in fluorescence emission from blue to greenish-yellow upon interaction with GSH, attributable to the cleavage of **NAPB** to its parent fluorophore, **NCB**. Additionally, **NAPB** exhibits a relatively linear response to GSH concentration within a range of 0 to 10 equivalents and establishes a detection limit as low as 39.1 nM. The probe also showcases a rapid response time of 5 to 10 min for comprehensive GSH detection and maintains substantial pH stability within the physiological range (4 to 8). MTT assays conducted in HepG2, HCT116 and MCF7 cancer cells validate the biosafety of the probe, revealing greater than 90 % cell viability at concentrations of up to 5 μM. Moreover, fluorescence imaging in HepG2 cells further substantiates the potential of **NAPB** as an exceptional tool for the detection of GSH in living cells. This study not only highlights the probe's applicability in advancing research related to GSH-associated disease diagnoses but also lays the foundation for the conceptualization and development of other innovative fluorescent probes aimed at GSH or other biothiol detection. Furthermore, our laboratory is currently focused on optimizing the fluorophore (**NCB**) emission to the near-infrared region (NIR) of the spectrum (650–700 nm) to create probes suitable for *in vivo* applications and future utilization in diseased animal models.

4. Experimental section

1. Materials and methods.

All chemicals were purchased from TCI Chemicals and Spectrochem Ltd, and used as received. Molychem silica gel (60–120 mesh) was used for column chromatography, and thin-layer chromatography was performed on Merck pre-coated silica gel 60-F254 plates. All other chemicals and solvents were obtained from commercial sources and purified using standard methods. The ^{1}H NMR and ^{13}C NMR spectra were recorded on Bruker-Advance 600 MHz spectrometers. Chemical shifts (δ) are reported in parts per million (ppm), using TMS (δ = 0) as an internal standard and d^6-DMSO as NMR solvent. The mass spectrum of the compounds has been obtained by Waters Q-ToF Premier Mass Spectrometer. UV absorbance was measured on Agilent Cary UV 60 UV–Visible Spectrophotometer. Fluorescence data were recorded on a Molecular Devices SpectraMax M5 multimode plate reader. Solvent used for fluorescence spectra: PBS, 1X (SRL Chemicals). GraphPad Prism ver. 7.0a (GraphPad Software, Inc.) and Origin2017 softwares were used to analyze data and generate graphs. Human colon cancer cells (HCT-116), breast cancer cells (MCF-7) and hepatocarcinoma cells (HepG2) were procured from the National Center for Cell Science (NCCS), Pune, India. DMEM (Dulbecco's Modified Eagle Medium) was chosen as the cell culture medium and was purchased along with 12-well cell culture plates from Genetics (Genetics Biotech Asia Pvt. Ltd). The T-25 flasks and 96 well plates were purchased from Eppendorf. Other growth media essentials, such as Streptomycin, Penicillin, Trypsin-EDTA, and Fetal Bovine Serum (FBS) were purchased from Gibco. Phosphate Buffer Saline (PBS) was prepared using high-grade analytical chemicals. The cells were cultured in FBS and penicillin-streptomycin supplemented DMEM and grown in a humidified CO_2 incubator at 37 °C.

2. Step-wise synthesis of probe NAPB.

a. Procedure of synthesis of precursor B: A 10 ml round bottomed flask was charged with 6-bromo-1*H*,3*H*-benzo[de]isochromene-1,3-dione (**A,** 0.825 g, 3 mmol) and *n*-butylamine (2.5 equiv.) in ethanol (5 mL) as solvent and refluxed at 80 °C for 2 h After cooling the reaction mixture to ambient temperature, the solvent was evaporated *in vacuo* and the crude mixture was then diluted with water (10 mL) and extracted with ethyl acetate (15 mL ×3). After drying with anhydrous Na_2SO_4, the organic phase was evaporated to dryness and purified by column chromatography using 15 % ethyl acetate: hexane as eluent to yield **B** (75 % yield) as a white solid.

b. Procedure of synthesis of NCB: Compound **B** (0.3 mmol, 1 equiv.) and cyclobutylamine (1.5 equiv.) were weighed and placed in a 25 ml round bottomed flask containing 2 mL of DMSO. To this mixture triethylamine (1.5 equiv.) was added as a base and the reaction mixture was stirred at 110 °C for 6 h After cooling the reaction mixture to ambient temperature, the crude mixture was then diluted with water (10 mL) and extracted with ethyl acetate (10 mL ×3). After drying with anhydrous Na_2SO_4, the organic phase was evaporated to dryness and purified by column chromatography using 15 % ethyl acetate: hexane as eluent to yield **NCB** as a yellow crystalline solid (78 % yield).

c. Procedure of synthesis of NAPB: NCB (0.5 mmol) and dried Na_2CO_3 (2 equiv.) were taken in ACN (1.5 mL) as solvent in a 25 mL reaction flask and stirred at 0 °C on an ice bath. To the slurry, a solution of chloroacetyl chloride (5 eq.) in 1.5 mL of ACN was added dropwise and the reaction mixture was then refluxed at 80 °C for 2 h As soon as the yellow fluorescence of **NCB** disappeared, the reaction mixture was brought to room temperature and diluted with water (25 mL) and extracted with ethyl acetate (10 mL ×3). After drying with anhydrous Na_2SO_4, the organic phase was evaporated to dryness and purified by column chromatography using 18 % ethyl acetate: hexane as eluent to yield **NAPB** as a yellow liquid (76 % yield).

3. Reaction of NAPB with biothiols (GSH and Cys): A 5 mL glass vial charged with **NAPB** (0.012 mmol) dissolved in DMSO (100 μL) was stirred with dropwise addition of biothiols (GSH and Cys) (1 equiv.) and catalytic amount of dried Na_2CO_3 (to maintain pH at 8.5) dissolved in water (100 μL) at ambient temperature and open-air conditions for 30 mins. The pH of the reaction mixture was monitored at regular intervals with pH paper. The selectivity experiment was carried out using an equimolar mixture (1:1) of GSH:Cys in water in place of GSH/Cys in the above-mentioned reaction protocol and the reaction was carried out for 1 h

4. Control experiment with *N*-Propylmaleimide (NPM): In a glass vial (5 mL), NPM (1 equiv.), GSH (1 equiv.) and dried Na_2CO_3 (1.5 equiv.) were added in sequence and dissolved in water (100 μL) with continuous stirring at room temperature. After 10 mins, **NAPB** (0.012 mmol) dissolved in DMSO (100 μL) was added to the reaction mixture and stirred at ambient temperature and open-air conditions for another 30 mins.

5. UV–VIS and fluorescence measurements of probe NAPB.

The stock solution of probe **NAPB** (100 μM) was made in 25 mM PBS mixed with DMSO in a ratio of 8:2 (pH 7.4). It was then diluted to 1.25 μM concentration using PBS and used freshly. The stock solutions of GSH (100 μM) and Cys (100 μM) were prepared in PBS and then diluted to serial concentrations ranging between 0 and 20 equivalents w.r.t. **NAPB** (1.25 μM) and used freshly. The absorption and emission wavelengths of

the resultant solution of the probe were measured in the absence and in the presence of GSH in PBS (1 equiv.) and plotted into graphs. For pH stability study, the buffers having pH ranges 4–8 were prepared using deionized water following standard protocol and freshly used. Probe **NAPB** (20 μM) was placed in each buffer system and incubated for 30 mins at 37 °C before measuring the fluorescence intensities. Stock solutions (100 μM) of Na^+, K^+, Fe^{3+}, Cl^-, HCO_3^-, Glu, Gly, His, Arg. l-Cys, *N*-Ac-Cys and GSH were prepared respectively in deionized water and used freshly. Stock solutions (100 μM) of HOONO ($OONO^-$) and H_2O_2 were prepared immediately before use. Fluorescence spectra were obtained 90 mins after mixing at 37 °C [18].

6. *In vitro* cytotoxicity testing of NAPB using MTT assay.

Cytotoxicity of probe **NAPB** against HepG2 cell lines was analyzed in a 96-well cell culture plate, which contained 1×10^4 cells/well. The cells were distributed such that each well contained 100 μL of the complete culture medium. The culture plate was then placed in a CO_2 incubator with 5 % CO_2 at 37 °C for 24 h to allow cell adherence. After 24 h of incubation, the media was aspirated, and fresh media was added comprising of probe **NAPB** at different concentrations within a range of 1 - 10 μM and incubated for another 24 h After 24 h, media was aspirated, and fresh media containing of MTT (3-(4,5-dimethylthiazol-2-yl)−2,5-diphenyltetrazolium bromide) was added to each well and incubated for an additional 2 h at 37 °C. The MTT-containing media was then aspirated, and 100 μL of DMSO was added to each well and subsequently incubated for another 30 mins to dissolve the formazan precipitate. The plate was incubated for the next 10 mins with gentle shaking. The optical density of each well was measured at 570 nm using a microplate reader. A similar cytotoxicity assay protocol was followed in the case of the other two cell lines, namely, HCT-116 and MCF-7 cells.

7. Fluorescence imaging of NAPB-treated HepG2 cells.

Hep G2 cells were seeded in a 12 well culture plate at 3×10^4 cells/well density and incubated overnight in a CO_2 incubator with 5 % CO_2 at 37 °C to obtain cell adherence. After 24 h of incubation, the media was aspirated, and fresh media was added containing 5 μM **NAPB** for 1 h Next, probe treated cells in four of these wells were incubated with GSH (5 μM) and other four were incubated with a GSH:NPM mixture (5 μM each) for another 30 mins. After completion of treatment, cells were washed with cold PBS three times, and images were captured using an inverted fluorescence microscope in the blue channel (λ_{abs}: 357/44 nm and λ_{em}: 447/60 nm) at 400 X magnification.

Author contribution statement.

S.D. performed the synthesis, structural characterization and photophysical studies of the probe. P.G. performed the biological assays. H. K.I. performed the time-based analysis of probe. B.K. designed the biological studies. D.K.S. supervised the work. The manuscript was written through the contributions of all authors.

Data Availability

All the synthetic procedures and spectral data are provided in the supplementary material of the manuscript.

CRediT authorship contribution statement

Samarpita Das: Writing – original draft, Investigation, Formal analysis, Data curation. **Pooja Goswami:** Investigation. **Harish K. Indurthi:** Formal analysis, Data curation. **Biplob Koch:** Resources, Methodology, Funding acquisition. **Deepak K. Sharma:** Writing – review & editing, Supervision.

Declaration of competing interest

The authors declare no competing financial interests or personal relationships.

Acknowledgement

D.K.S. thanks the Department of Biotechnology (DBT), India (102/IFD/SAN/3016/2019–20) for financial support. B.K. acknowledges Banaras Hindu University for providing funding under the IoE scheme (file no. R/Dev/D/IoE/Incentive/2021-22/32449). S.D. thanks the Department of Science and Technology (DST), Govt. of India for providing DST-INSPIRE fellowship (IF190906).

Supplementary materials

Supplementary material associated with this article can be found, in the online version, at doi:10.1016/j.molstruc.2025.141490.

Data availability

I have shared the data in Attach files section

References

[1] G. Calabrese, B. Morgan, J. Riemer, Mitochondrial Glutathione, Regulation and functions, Antiox. Redox Signal. 27 (2017) 1162–1177, https://doi.org/10.1089/ars.2017.7121.
[2] H.J. Forman, H. Zhang, A. Rinna, Glutathione: overview of its protective roles, measurement, and biosynthesis, Mol. Asp. Medi. 30 (2009) 1–12, https://doi.org/10.1016/j.mam.2008.08.006.
[3] H. Sies, Glutathione and its role in cellular functions, Free rad, Biol. Medi. 27 (1999) 916–921, https://doi.org/10.1016/S0891-5849(99)00177-X.
[4] S.J. Kim, H.S. Kim, Y.R. Seo, Understanding of ROS-inducing strategy in anticancer therapy, Oxid. Med. Cell. Longev. (2019) 5381692, https://doi.org/10.1155/2019/5381692, 2019.
[5] D.P. Jones, [11]Redox potential of GSH/GSSG couple: assay and biological significance, in: H. Sies, L. Packer (Eds.), Met. Enzymol., Academic Press, 2002: pp. 93–112. 10.1016/S0076-6879(02)48630-2.
[6] F.J. Giblin, Glutathione: a vital lens antioxidant, J. Ocul. Pharmacol. Ther. 16 (2000) 121–135, https://doi.org/10.1089/jop.2000.16.121.
[7] X. Tian, L.K. Kumawat, S.D. Bull, R.B.P. Elmes, L. Wu, T.D. James, Coumarin-based fluorescent probe for the detection of glutathione and nitroreductase, Tetrahedron 82 (2021) 131890, https://doi.org/10.1016/j.tet.2020.131890.
[8] L. Wu, X. Tian, R.R. Groleau, J. Wang, H.-H. Han, S.B. Reeksting, A.C. Sedgwick, X.-P. He, S.D. Bull, T.D. James, Coumarin-based fluorescent probe for the rapid detection of peroxynitrite 'AND' biological thiols, RSC Adv 10 (2020) 13496–13499, https://doi.org/10.1039/d0ra02234a.
[9] S. Das, H.K. Indurthi, P. Asati, P. Saha, D.K. Sharma, Benzothiazole based fluorescent probes for the detection of biomolecules, physiological conditions, and ions responsible for diseases, Dyes Pigm 199 (2022) 110074, https://doi.org/10.1016/j.dyepig.2021.110074.
[10] S. Das, H.K. Indurthi, P. Saha, D.K. Sharma, Coumarin-based fluorescent probes for the detection of ions, biomolecules and biochemical species responsible for diseases, Dyes Pigm 228 (2024) 112257, https://doi.org/10.1016/j.dyepig.2024.112257.
[11] F. Yan, J. Sun, Y. Zang, Z. Sun, H. Zhang, X. Wang, Benzothiazole applications as fluorescent probes for analyte detection, J. Iran. Chem. Soc. 17 (2020) 3179–3203, https://doi.org/10.1007/s13738-020-01998-9.
[12] M. Cao, H. Chen, D. Chen, Z. Xu, S.H. Liu, X. Chen, J. Yin, Naphthalimide-based fluorescent probe for selectively and specifically detecting glutathione in the lysosomes of living cells, Chem. Commun. 52 (2015) 721–724, https://doi.org/10.1039/C5CC08328A.
[13] J. Ou-Yang, C.-Y. Li, Y.-F. Li, J. Fei, F. Xu, S.-J. Li, S.-X. Nie, A rhodamine-based fluorescent probe with high water solubility and its application in the detection of glutathione with unique specificity, Sens. Actuators Chem. 240 (2017) 1165–1173, https://doi.org/10.1016/j.snb.2016.09.074.
[14] H. Li, Y. Yang, X. Qi, X. Zhou, W.X. Ren, M. Deng, J. Wu, M. Lü, S. Liang, A. T. Teichmann, Design and applications of a novel fluorescent probe for detecting glutathione in biological samples, Anal. Chim. Acta 1117 (2020) 18–24, https://doi.org/10.1016/j.aca.2020.03.040.
[15] X. Qi, L. Shang, S. Liang, H. Li, J. Chen, C. Xin, J. Zhao, M. Deng, Q. Wang, Q. He, M. Lv, A.T. Teichmann, Z. Wang, Y. Yang, Development and applications of a coumarin-based "turn-on" fluorescent probe for effectively discriminating reduced glutathione from homocysteine and cysteine in living cells and organisms, Dyes Pigm 194 (2021) 109625, https://doi.org/10.1016/j.dyepig.2021.109625.
[16] S. Das, P. Goswami, V.K. Verma, H.K. Indurthi, M. Kumar, B. Koch, D.K. Sharma, Rapid access to 7-substituted cycloalkylamino and alkylamino analogues of 4-methylcoumarin reveals surprising emitters, Dyes Pigm 217 (2023) 111407, https://doi.org/10.1016/j.dyepig.2023.111407.
[17] S. Das, P. Goswami, H.K. Indurthi, B. Koch, D.K. Sharma, Improving the fluorescence brightness of naphthalimide and nitrobenzoxadiazole dyes with cycloalkylamine auxochromes, Dyes Pigm 227 (2024) 112206, https://doi.org/10.1016/j.dyepig.2024.112206.
[18] S. Das, A. Chaudhuri, H.K. Indurthi, A.K. Agrawal, D.K. Sharma, Azacoumarin-based "turn-on" fluorescent probe for the detection and imaging of hydrogen peroxide in living cells, Org. Biomol. Chem. 22 (2024) 7332–7336.